Revista Brasileira de Geofísica
RBGf
Brazilian Journal of Geophysics

Revista Brasileira de Geofísica (2004) 22(1): 17-32

ISSN 0102-261X
www.scielo.br/rbg

AN ALTERNATIVE EXPERIMENTAL METHOD TO DISCRIMINATE MAGNETIC PHASES USING IRM ACQUISITION CURVES AND MAGNETIC DEMAGNETISATION BY ALTERNATING FIELD

Marcos A.E. Chaparro[1] and Ana M. Sinito[2]

Recebido em 04 fevereiro, 2004 / Aceito em 23 julho, 2004
Received February 04, 2004 / Accepted July 23, 2004

ABSTRACT. Separation of different magnetic phases in natural samples composed by a mix of several magnetic minerals become necessary in rock magnetism in order to identify and describe the main magnetic carriers. However, this task may be difficult to carry out successfully.

The goal of the proposed method in this paper is to determine and discriminate *experimentally* magnetic (soft and hard) phases in synthetic and natural samples. The present method uses two different magnetic techniques, isothermal remanent magnetisation acquisition and magnetic demagnetisation alternately. After the entire process of induced remanent magnetisation and demagnetisation is performed, three residual isothermal remanent magnetisation curves are obtained. This discrimination is achieved by using as *filters (sorter)* different peak values for alternating demagnetising fields.

Well-known pure and mixed synthetic iron oxides (magnetite and hematite) were firstly studied to investigate and corroborate the reliability of our experimental method, obtaining successful results. Subsequently, natural samples containing soft and hard minerals (magnetite, hematite, goethite, etc.) from stream-sediments, soils and a mine were also studied.

Comparisons with other purely numerical methods were carried out, yielding a good agreement among them. Our method is more time-consuming than others, but separation of individual magnetic curves is achieved by an experimental procedure, which is more realistic. It is also possible to apply this method to backfield isothermal remanent magnetisation measurements obtaining valuable information of H_{CR} and S-ratio for each phase.

Keywords: Magnetic phases discrimination, Isothermal Remanent Magnetisation, Magnetic demagnetisation by AF, remanence coercivity, synthetic iron oxides.

RESUMEN. La separación de distintas fases magnéticas en muestras naturales, compuestas por diferentes minerales magnéticos, se ha vuelto necesaria en magnetismo a fin de identificar y describir los principales portadores. Sin embargo, esta tarea puede ser difícil de llevar a cabo.

El objetivo del método propuesto es determinar y discriminar *en forma experimental* fases magnéticas en muestras sintéticas y naturales. El método usa dos técnicas magnéticas diferentes en forma alternada, adquisición de magnetización remanente isotérmica y desmagnetización magnética. Una vez concluido el proceso de mediciones de magnetización remanente inducida y desmagnetización magnética, usando como *filtro (clasificador)* diferentes valores pico de campo alterno para la desmagnetización magnética, se obtienen tres curvas de magnetización remanente residual. Es también posible aplicar este método a mediciones de magnetización remanente isotérmica de campo reverso obteniendo información valiosa de los parámetros H_{CR} y S-ratio para cada fase.

Oxidos de hierro sintéticos puros y mezclados (magnetita y hematita) fueron primeramente estudiados para investigar y corroborar la confiabilidad de nuestro método experimental, obteniendo los resultados esperados. En segundo término, se estudiaron muestras naturales conteniendo distintos minerales (hematita, goethita, magnetita, etc.).

Finalmente, se llevaron a cabo comparaciones con otros métodos puramente numéricos, obteniendo un buen acuerdo con ellos. Nuestro método es más costoso en tiempo, no obstante, la separación es lograda por medio de un procedimiento experimental, el cual es más realista.

Palabras-clave: Discriminación de fases magnéticas, magnetización remanente isotérmica, desmagnetización magnética usando AF, coercitividad de remanencia, óxidos de hierro sintéticos.

[1]IFAS, Universidad Nacional del Centro de la Provincia de Buenos Aires, Pinto 399, 7000 Tandil, Argentina – Tel: +54 2293 444432, Fax: +54 2293 444433 – E-mail: chapator@exa.unicen.edu.ar

[2] IFAS, Universidad Nacional del Centro de la Provincia de Buenos Aires, Pinto 399, 7000 Tandil, Argentina – Tel: +54 2293 444432, Fax: +54 2293 444433 – E-mail: asinito@exa.unicen.edu.ar

INTRODUCTION

Isothermal Remanent Magnetisation (IRM) acquisition is very sensitive to the presence of diverse assemblages of magnetic grains; however, it is difficult to distinguish different magnetic phases from a natural sample composed by a mix of several magnetic minerals.

The most popular methods to separate the magnetic component use the gradient of experimental IRM curve (e.g. Robertson and France, 1994; Stockhausen, 1998; Kruiver et al., 2001a and 2001b, Heslop et al., 2002). It is possible to model the IRM curve, although often there is more than one possible solution. If this is the case, additional background information is needed to remove the non-uniqueness and to obtain correct interpretations. Other methods for discriminating magnetic mineralogy, based on parameters related to IRM acquisition (SIRM and remanent coercivity), are plots of Thompson and Oldfield (1986), biplots of Peters and Thompson (1998), flowcharts of Maher et al. (1999) and biplots of Peters et al. (2002).

Magnetic parameters derived from IRM acquisition measurements are closely influenced by predominant magnetic carriers. The influence and features of non-predominant magnetic carriers to bulk response can be mashed by the dominant ones and therefore they cannot always be differentiated.

In this paper, an experimental method to find and discriminate various magnetic phases is proposed. The main tools used in this method are IRM acquisition and magnetic demagnetisation techniques. Parameters and curves obtained from these techniques are related to grain size and mineralogy of magnetic carriers, so both measurements can be jointly used to find out several magnetic phases.

The main aim of this tool is to provide an experimental and therefore realistic discrimination of magnetic phases.

SAMPLES

Synthetic and natural samples

We study synthetic and natural materials. Synthetic iron oxides of magnetite (Fe_3O_4) and hematite (Fe_2O_3) from Bayferrox®, labelled MgSth2 and HmSth respectively, were prepared and their magnetic properties were investigated in the laboratory. The magnetite is a black powder and according to electron micrographs, its particles are spherical and the maximum grain size is 0.2μm. In the case of hematite, it is a red powder, its particles are acicular and the maximum grain size is $0.1 \times 0.8\mu$m.

According to the Bayferrox® Company, synthetic magnetite contains approximately 90% of Fe_3O_4; synthetic hematite contains between 97 and 98% of Fe_2O_3. Minute traces of ferrimagnetic materials were detected in our IRM preliminary studies of pure hematite (item 4, Fig. 3); thermal studies confirmed this result. This ferrimagnetic phase was also detected in synthetic hematites in other studies (de Boer and Dekkers, 1998; France and Oldfield, 2000). The material was thermally treated in order to remove (minimise) the ferrimagnetic phase (possibly magnetite or maghemite) without affecting the hematite; it was heated in air up to $750°$C. After this process, a new sample, HmSth3, was prepared by using the treated material. Two other samples were also prepared mixing different proportions of thermally treated hematite and magnetite: HmMgSth1, 420 parts of hematite per one part of magnetite (420:1) and HmMgSth2, 110 parts of hematite per one part of magnetite (110:1).

The natural samples were collected from different environments. Two samples (PE1a8 and PE1a12) were obtained from stream-sediments (La Plata, Argentina), belonging to different depths and therefore with different magnetic characteristics. One sample (GoP2) belongs to a soil from La Plata (Argentina), and the other sample of natural goethite (Goeth1b) was taken out from Tharsis (Spain). Exhaustive analysis on these samples were carried out by Chaparro et al. (2002a, 2002b and 2003).

THE METHOD

The method is based on the responses of different assemblages of magnetic materials when they are subject to a pulse magnetising field and a demagnetising AF. From both studies, useful curves and magnetic parameters are achieved and therefore bulk data about magnetic carriers can be obtained, although only *qualitative* information of individual magnetic population can be inferred. However, numerical methods applied to IRM acquisition curves (Kruiver et al, 2001a; Heslop et al., 2002) have been successful developed in order to get a quantitative separation of bulk IRM curve into individual IRM contributing curves.

In this work an alternative method is proposed in order to split *experimentally*, and therefore in a more realistic way, the bulk IRM curve into individual magnetic phases. The separation of magnetic phases is achieved by using IRM acquisition and AF demagnetisation alternately. After each magnetisation step, two consecutive AF demagnetisation are performed, so a bulk remanent magnetisation and two residual remanent magnetisations are measured at each stage of the method. Thus, the separation may be achieved using different AF demagnetisation peak values as *filters (sorter)*, in this work we use only two peak values. These peak AF values are specially chosen according to the marked different response of soft and hard magnetic materials.

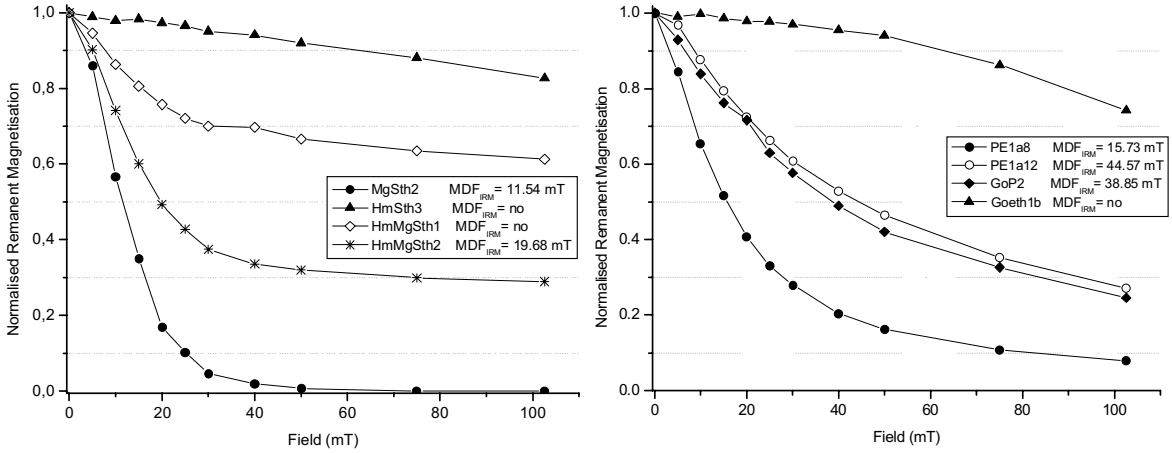

Figure 1 – Demagnetisation of SIRM curves for Synthetic (MgSth2, HmSth3, HmMgSth1 and HmMgSth2) and Natural samples (PE1a8, PE1a12, GoP2 and Goeth1b).
Figura 1 – *Curvas de demagnetización de MRIS de muestras sintéticas (MgSth2, HmSth3, HmMgSth1 y HmMgSth2) y naturales (PE1a8, PE1a12, GoP2 y Goeth1b).*

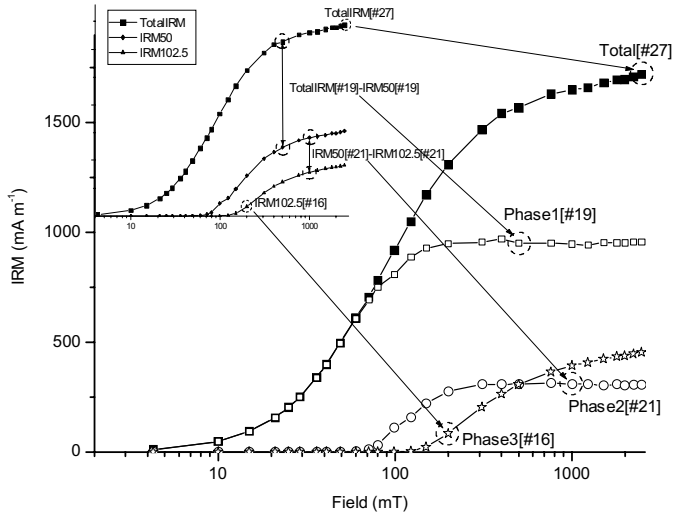

Figure 2 – Total and Phases IRM acquisition curves obtained from equations 1a-c. (Inset) measured data points, TotalIRM measurements, and residual remanent magnetisation measurements (IRM50 and IRM102.5) are shown. Differences between measured remanent magnetisation (e.g. TotalIRM[#19]-IRM50[#19]) for two growing DC field steps (#19 and #21) and their corresponding results (e.g. Phase1[#19]) are shown. The direct relation between Total and Phase3 and TotalIRM and IRM102.5 curves is also shown, e.g. Phase3[#16]=IRM102.5[#16].

Figura 2 – *Curvas de MRI de adquisición Totales y Fases obtenidas de las ecuaciones 1a-c. En el recuadro, se muestran los puntos medido, mediciones de MRITotal, y mediciones de magnetización remanente residual (MRI50 y MRI102.5). Pueden apreciarse en el gráfico las diferencias entre magnetizaciones remanentes medidas (por ej.: MRITotal[#19] - MRI50[#19]) para dos etapas de campo DC creciente (#19 y #21) y sus correspondientes resultados (por ej.: Fase1[#19]). Se muestra también, la relación directa entre las curvas Total y Fase3, con MRITotal y MRI102.5 (por ej.: Fase3[#16] = MRI102.5[#16]).*

Residual remanent magnetisation curves and discrimination of IRM phase curves

Under low fields (AF $\sim$ 50 mT) magnetic assemblages with predominance of soft materials are almost completely demagnetised; on the other hand, harder materials do not show significant decrease of the remanent magnetisation (e.g. Dankers, 1978; Dankers, 1981; Bailey and Dunlop, 1983; Xu and Dunlop, 1995; Argyle et al., 1994; Dunlop and Özdemir, 1997). Dankers (1978) carried out studies on magnetites, maghemites, titanomagnetites and hematites. Demagnetisation curves from these studies and measurements carried out on our synthetic magnetite samples (Fig. 1) show that soft magnetic materials like magnetites are almost entirely demagnetised at a peak AF of 50 mT, although titanomagnetites and maghemite and very fine grained magnetite show a small residual remanent magnetisation. Fine hematites ($< 20\mu$m, Dankers, 1978) and also our synthetic hematite (Fig. 2) were

in most cases, not significantly affected by higher AF (100 mT). However, it must be taken into account that remanent magnetisation is partially reduced, in some cases up to 20% or more according to the kind of hematite and its grain size.

This fact can be useful if it is used as a *filter (sorter)* method between soft and hard magnetic phases. In this work we chose two peaks AF as *AF filters*, which were set at 50 mT (moderate filter) and 102.5 mT (relatively strong filter) with the aim of discriminating material with different coercive forces.

Each sample was magnetised using a pulse magnetiser model IM-10-30 ASC Scientific in 27 growing DC field steps (from 4.3 to 2470 mT) and three measurements were taken in each step with a spinner fluxgate magnetometer Minispin, Molspin Ltd. After each magnetisation step, remanent magnetisation (Total IRM (#i), i indicates the magnetisation step) was measured. The sample was then demagnetised using 50 mT as peak value and its residual remanent magnetisation was measured (named IRM50 (#i), i indicates the magnetisation step). Magnetic demagnetisation by the *tumbling method* was carried out using the Shielded Demagnetiser Molspin Ltd. *Reversing option* was chosen, allowing the direction of tumbling to be reversed every four rotations, and a decay rate of the peak AF of 17μT per cycle was set. Finally, the sample was demagnetised using a higher peak value (102.5 mT) and the new residual remanent magnetisation was measured (named IRM102.5 (#i) i indicates the magnetisation step). This process was carried out until saturation (i = 1 to 27, DC field for the 27^{th} step is 2470 mT) was reached (Saturation IRM, SIRM). At saturation three remanent magnetisations were measured; they are IRM(#27), named Total SIRM; IRM50(#27), named SIRM50; and IRM102,5(#27), named SIRM102.5. Total IRM curves and IRM for three different magnetic phases obtained by subtraction may be drawn,

$$Phase3(\#1) = IRM102.5(\#i) \quad (1a)$$

$$Phase2(\#1) = IRM50(\#i) - IRM102.5(\#i) \quad (1b)$$

$$Phase1(\#1) = TotalIRM(\#i) - IRM50(\#i) \quad (1c)$$

Residual remanent magnetisation, Total and Phase curves are shown on Fig. 2; differences between residual curves at two different field steps (i = 19 and i = 21) and their corresponding results (data point from Phase1(#19), Phase1(#21) and Phase2(#19), Phase2(#21)) are also shown.

Phase 1 is the softest one (AF < 50 mT), Phase 2 is median (50 mT $<$ AF $<$ 102.5 mT) and Phase 3 is the hardest one (AF > 102.5 mT). From this discrimination it is possible to find every Phase SIRM and its corresponding magnetic contribution (%) to the Total SIRM. These percentages represent the contribution to the remanent magnetisation (magnetic signal) and they are not (necessarily) directly related to the concentration of magnetic materials because all minerals (magnetite, hematite, goethite, etc.) also depend on magnetic features.

This method can also be applied to backfield measurements, although this process must be carried out separately for each demagnetising peak AF value. From Total SIRM, SIRM50 and SIRM102.5 backfield measurements are obtained. A residual backfield IRM curve is entirely achieved using only a determined peak AF value; after the process is finished another residual backfield IRM curve using another peak AF value is measured.

Finally, several magnetic parameters, remanent coercitivity (H_{CR}), remanent acquisition coercitivity ($H_{1/2}$), and S-ratio ((1-IRM-$_{300mT}$/SIRM)/2, according to Bloemendal et al., 1992) from this magnetic discrimination can be estimated. From demagnetisation curves the median destructive fields (MDF) were calculated.

MEASUREMENTS AND RESULTS

Total IRM measurements and the three Phases obtained for the different magnetic phases are displayed for each sample in Fig. 3, 4 and 5. Measured and calculated values for several related IRM parameters are listed in Tables 1 and 2.

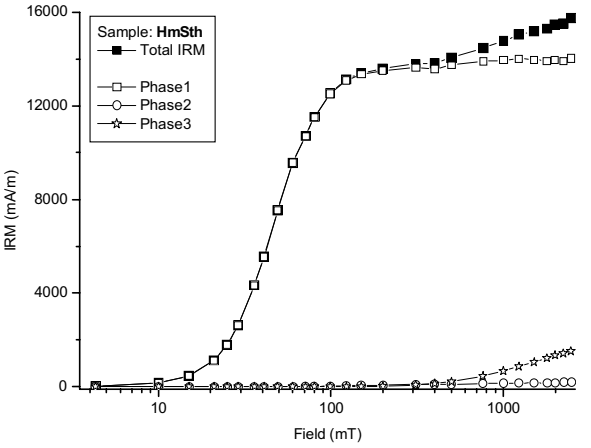

Figure 3 – Total and Phases IRM acquisition for thermally untreated synthetic hematite, HmSth sample.

Figura 3 – *Curvas de MRI de adquisición Total y Fases para hematita sin tratar térmicamente, muestra HmSth.*

As it was mentioned in item 2.1, preliminary studies of IRM acquisition for synthetic samples were carried out to test their magnetic properties. In the HmSth sample a high SIRM was observed; this Total SIRM is dominated by a soft phase, although a reduced hard phase is also present (Table 1 and Fig. 3).

Magnetic measurements for synthetic samples showed differences according to their concentration (Fig. 4). Total SIRMs of "pure" samples, MgSth2 and HmSth3, are distinctively different. Total SIRM (and specific SIRM) values for mixed samples, HmMgSth1 and HmMgSth2, were similar (Table 1).

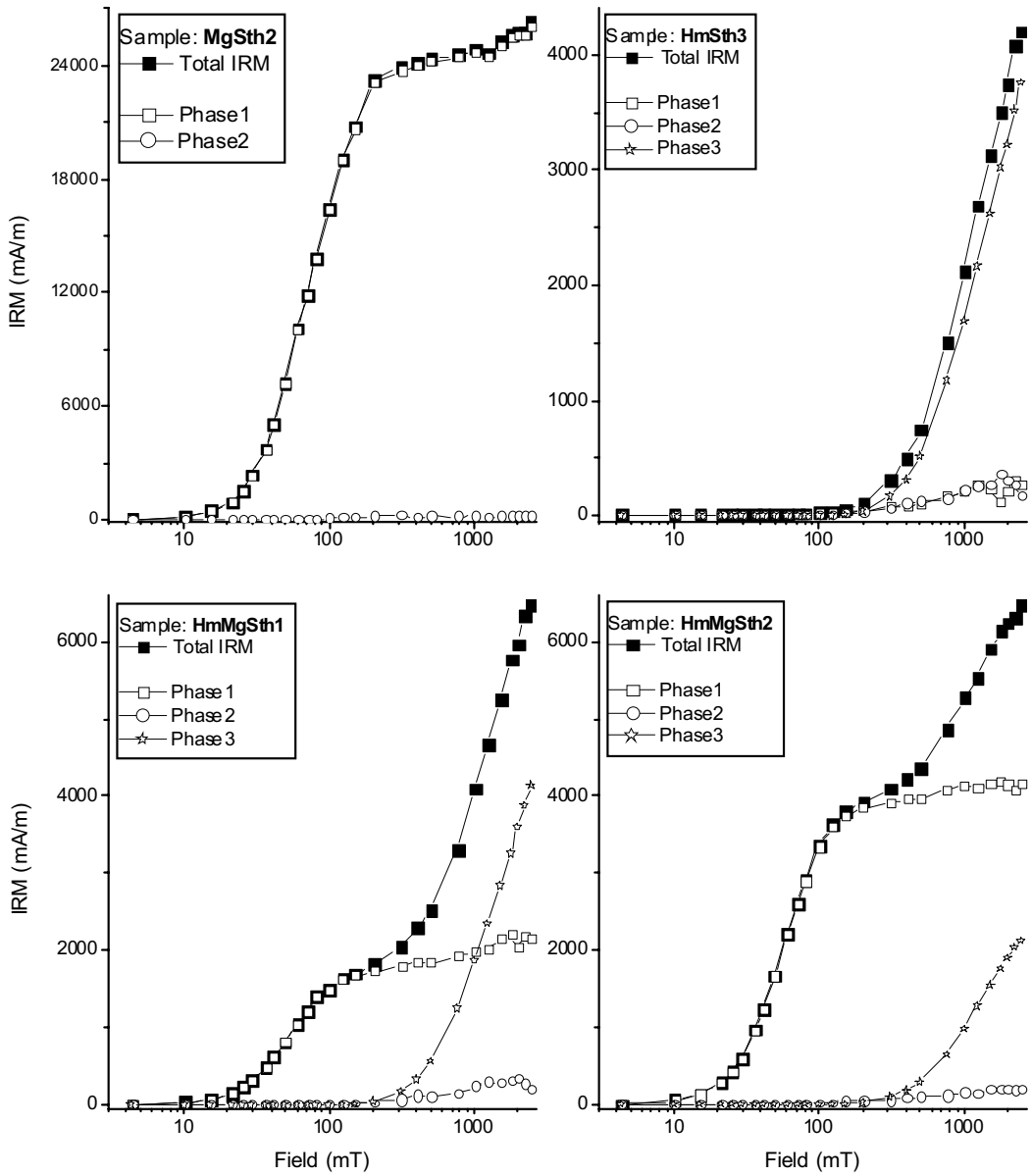

Figure 4 – Total and Phases IRM acquisition for synthetic samples. "Pure"samples are MgSth2 (magnetite) and HmSth3 (thermal treated hematite); mixed samples are HmMgSth1 (420 parts of hematite per 1 of magnetite) and HmMgSth2 (110 parts of hematite per 1 of magnetite)

Figura 4 – *Curvas de MRI de adquisición Total y Fases para las muestra sintéticas. Las muestras "puras"son MgSth2 (magnetita) y HmSth3 (hematita térmicamente tratada); las muestras mezcla son HmMgSth1 (420 partes de hematita por 1 de magnetita) y HmMgSth2 (110 partes de hematita por 1 de magnetita).*

Total SIRM (and specific SIRM) of the two stream-sediment samples (PE1a8 and PE1a12) are very different. GoP2 and Goeth1b samples also showed differences (Table 2 and Fig. 5).

$H_{1/2}$ was calculated from Total IRM acquisition curves. High $H_{1/2}$ were found for synthetic samples with high content of hard materials (HmSth3 and HmMgSth1), and low $H_{1/2}$ for the other synthetic samples (MgSth2 and HmMgSth2) (Table 1). For natural samples, the lowest value belonged to PE1a8 sample and similar $H_{1/2}$ was found for PE1a12 and GoP2. On the other hand, the highest $H_{1/2}$ was found for Goeth1b sample (Table 2).

From backfield, H_{CR} were estimated (Fig. 6 and 7). They were in agreement with $H_{1/2}$ results for synthetic and natural samples as it can be observed in Tables 1 and 2.

S-ratio was also calculated for each sample. For synthetic

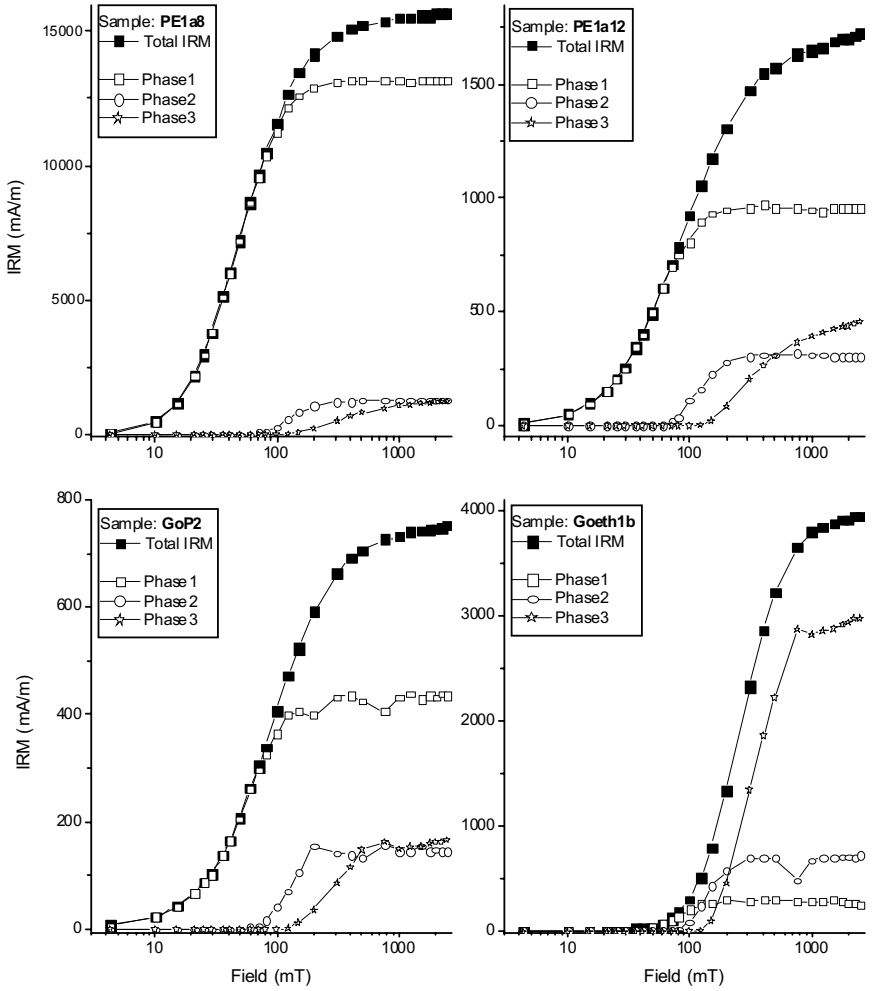

Figure 5 – Total and Phases IRM acquisition for natural samples. PE1a8 and PE1a12 were obtained from stream-sediments, GoP2 belongs to a soil, and Goeth1b is a sample of natural goethite.

Figura 5 – *Curvas de MRI de adquisición Total y Fases para las muestra naturales. Las muestras PE1a8 y PE1a12 fueron extraídas de sedimentos arroyo, la muestra GOP2 pertenece a un suelo, y Goeth1b es una muestra de goethita natural.*

samples, the highest value corresponds to MgSth2, and lower values were found for the other synthetic samples (Table 1). The highest value for natural samples corresponds to PE1a8 and Goeth1b sample has the lowest value (Table 2).

After demagnetisation with different peak AF values was applied, equations (1a-c) were used in order to calculate the three magnetic phases for each sample and their corresponding magnetic parameters (Fig. 4 and 5, Tables 1 and 2).

After IRM studies were done, additional measurements of demagnetisation of SIRM were made. Well-defined differences among demagnetisation curves and MDF parameter (MDF_{IRM}) are observed in Fig. 2. MDF_{IRM} was calculated from these curves and corresponding results are summarised in Tables 1 and 2. Extreme cases are MgSth2 (magnetite) and HmSth3 (hematite) synthetic samples, and PE1a8 (high content of natural magnetite) and Goeth1b (natural goethite) natural samples. The MDF_{IRM} was not reached for samples with high contents of hard magnetic materials (like as hematite and goethite), HmSth3, HmMgSth1 and Goeth1b samples.

DISCUSSION

Synthetic samples, pure and mixed iron oxides

As it was mentioned before, a soft (89.2%, $H_{1/2}$= 46.7 mT) and a hard phase (9.6%, $H_{1/2}$ = 1099.1 mT) were detected from preliminary studies carried out on HmSth. This soft phase was not expected in the hematite sample and it constitutes a contaminant not

Table 1. Several magnetic parameters from IRM acquisition, magnetic demagnetisation and the proposed method for synthetic samples.
Tabla 1. *Distintos parámetros magnéticos derivados de la MRI de adquisición, demagnetización magnética y el método propuesto para muestras sintéticas.*

Sample	Magnetic Parameters								
	Magnetic Phase	**Contribution** *(%)*	**SIRM** *(mA/m)*	**SIRM** *(Am^2kg^{-1})*	**H_{CR}** *(mT)*	**$H_{1/2}$** *(mT)*	**$H_{CR}/H_{1/2}$** *(dimensionless)*	**S-ratio** *(dimensionless)*	**MDF_{IRM}** *(mT)*
MgSth2 ("Pure" synthetic magnetite)	Total	100	26220	4.449	37.0	77.0	0.48	1.00	11.5
	1	99.4	26052		37.0	76.6	0.50	1.00	
	2	0.6	166		80.8	129.6	0.62	1.06	
HmSth3 ("Pure" synthetic hematite)	Total	100	4190	2.966E-2	889.5	992.1	0.90	0.14	--
	1	5.1	217		702.7	546.6	--	0.39	
	2	5.2	220		699.4	437.4	--	0.30	
	3	89.7	3757		931.9	1083.4	0.86	0.30	
HmSth (Thermally untreated synthetic hematite)	Total	100	15747	8.360E-2	--	50.6	--	--	--
	1	89.2	14041		--	46.7	--	--	
	2	1.2	189		--	353.0	--	--	
	3	9.6	1517		--	1099.1	--	--	
HmMgSth1 (Synthetic hematite and magnetite 420:1)	Total	100	6474	3.928E-2	605.5	737.0	0.82	0.38	--
	1	32.6	2115		37.9	58.9	0.61	0.85	
	2	3.4	223		829.2	391.2	--	0.30	
	3	64.0	4146		949.0	1091.8	0.87	0.30	
HmMgSth2 (Synthetic hematite and magnetite 110:1)	Total	100	6471	7.496E-2	57.2	94.0	0.61	0.69	19.7
	1	64.2	4157		33.1	57.6	0.57	0.96	
	2	3.0	192		360.0	527.8	--	0.38	
	3	32.8	2122		944.2	1055.1	0.89	0.38	

Table 2. Several magnetic parameters from IRM acquisition, magnetic demagnetisation and the proposed method for natural samples.
Tabla 2. *Distintos parámetros magnéticos derivados de la MRI de adquisición, demagnetización magnética y el método propuesto para muestras naturales.*

Sample	Magnetic Parameters								
	Magnetic Phase	**Contribution** *(%)*	**SIRM** *(mA/m)*	**SIRM** *(Am^2kg^{-1})*	**H_{CR}** *(mT)*	**$H_{1/2}$** *(mT)*	**$H_{CR}/H_{1/2}$** *(dimensionless)*	**S-ratio** *(dimensionless)*	**MDF_{IRM}** *(mT)*
PE1a8 (Sample from stream sediments, La Plata, Argentina)	Total	100	15656	1.405E-2	38.1	53.8	0.71	0.95	15.7
	1	84.0	13163		31.2	44.8	0.71	0.99	
	2	8.2	1289		122.4	133.3	0.92	0.96	
	3	7.8	1214		394.9	355.9	1.11	0.42	
PE1a12 (Sample from stream sediments, La Plata, Argentina)	Total	100	1719	1.500E-3	78.7	91.0	0.86	0.85	44.6
	1	55.3	951.4		38.6	47.6	0.81	0.99	
	2	18.3	314.0		119.8	123.3	0.97	0.99	
	3	26.4	455.2		329.2	342.6	0.96	0.45	
GoP2 (Sample from a soil, La Plata, Argentina)	Total	100	749.7	8.095E-4	77.5	90.4	0.86	0.88	38.8
	1	58.1	435.9		41.3	51.2	0.81	0.99	
	2	19.6	147.1		120.0	125.0	0.96	0.98	
	3	22.2	166.7		288.7	299.7	0.96	0.52	
Goeth1b (Natural goethite from Tharsis, Spain)	Total	100	3942	2.216E-2	272.0	270.7	1.00	0.56	--
	1	7.1	280		73.6	77.9	0.94	1.07	
	2	17.8	700		147.7	138.8	1.06	0.85	
	3	75.1	2961		325.8	333.3	0.98	0.43	

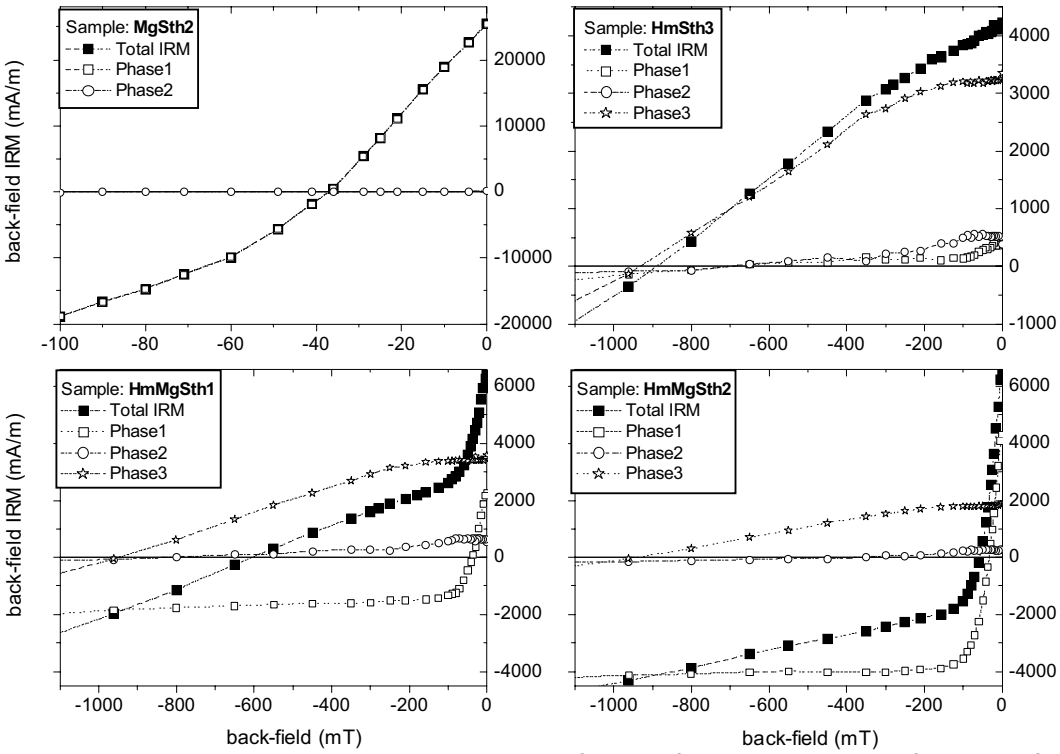

Figure 6 – Total and Phases backfield IRM for synthetic samples. Pure samples are MgSth2 and HmSth3; mixed samples are HmMgSth1 and HmMgSth2.

Figura 6 – *Curvas de MRI de backfield Total y Fases para las muestra sintéticas. Las muestras "puras" son MgSth2 y HmSth3 ; las muestras mezcla son HmMgSth1 y HmMgSth2.*

detected by the manufacturers (see item 2.1). Although the concentration of ferrimagnetic material is surely very low (minute traces) it is enough to dominate the remanent magnetisation (Fig. 3, Table 1).

The "pure" sample of thermally treated hematite, HmSth3, showed the same hard phase found in the sample of untreated hematite (HmSth), although in HmSth3 the contribution of the hard phase (89.7%, $H_{1/2}$ = 1083.4 mT) to Total IRM is predominant. This predominance is also reflected in its MDF_{IRM} that could not be reached.

Other (ferri)magnetic phases with relatively low contribution (5.1% and 5.2%) were also found (Fig. 4). Their presence may be due to a residual ferrimagnetic material that could not be completely removed or to some inaccuracy of the method when the percentage of contribution is too low. The last possibility seems to be more likely for this sample, if the parameters listed in Table 1 for soft and relatively soft phases are taken into account. This Table shows that H_{CR}s are too high and S-ratios are too low for this kind of phases, and that their values are also similar to the hard phase (Phase3).

An absolutely dominant soft phase (99.4%) for the other "pure" sample, MgSth2 was determined. According to the Total H_{CR}, S-ratio and MDF_{IRM}, 37.0 mT, 1.00 and 11.5 mT respectively, this phase clearly corresponds to a ferrimagnetic material, very probably pseudo-single-domain (PSD) magnetite. The Phase2 is not very reliable due to the low concentration (Table 1). However, the Phase2 H_{CR} could correspond to a small population of magnetite of finer grain size.

In order to test the discrimination ability of the method, it was applied in synthetic mixed samples where soft and hard phases with significant contribution were present. Measured specific SIRM for these mixtures (Table 1) are compared with predicted results calculated from the known ratios of the samples, 420:1 (HmMgSth1), 110:1 (HmMgSth2) and their corresponding SIRM values of "pure" magnetite (MgSth2) and hematite (HmSth3). Predicted results yield 4.027E-2 A m^2 kg^{-1} and 7.0204E-2 A m^2 kg^{-1} respectively, and are in agreement with measured values (Table 1) differing in between about 2.5% for HmMgSth1 and 6.3% for HmMgSth2.

Two phases, soft and hard, were successfully discriminated

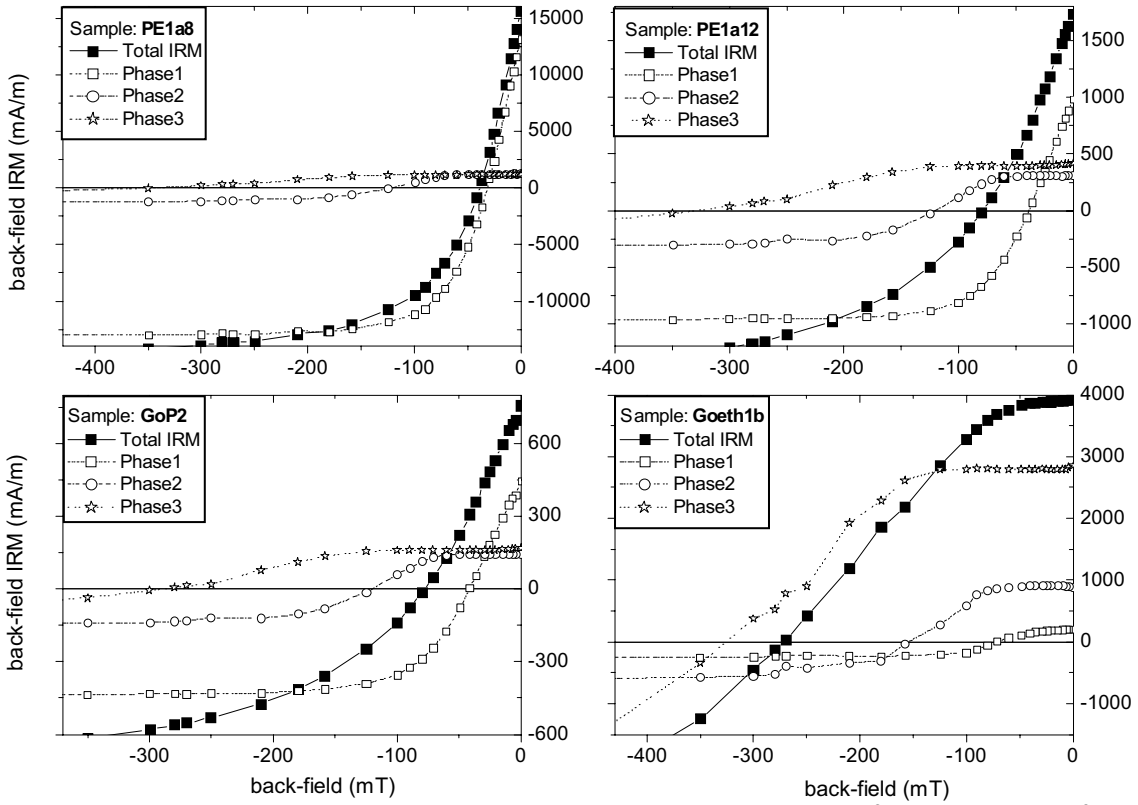

Figure 7 – Total and Phases backfield IRM for natural samples. PE1a8 and PE1a12 were obtained from stream-sediments, GoP2 belongs to a soil, and Goeth1b is a sample of natural goethite.

Figura 7 – *Curvas de MRI de adquisición Total y Fases para las muestra naturales. Las muestras PE1a8 y PE1a12 fueron extraídas de sedimentos arroyo, la muestra GoP2 pertenece a un suelo, y Goeth1b es una muestra de goethita natural.*

for HmMgSth1 and HmMgSth2 (Fig. 4), being both contributions in each sample in agreement with the proportion of hematite and magnetite used in their preparation (Table 1). The contribution of soft (Phase1) and hard (Phase3) phases were 32.6% and 64.0% for HmMgSth1 and inversely 64.2% and 32.8% for HmMgSth2. Predicted contributions of both soft and hard phases were also calculated and compared with the measured ones obtaining differences of about 6%.

The materials used for these samples were the same as the materials of the "pure" samples (HmSth3 and MgSth2), therefore, no dependent-concentration parameters must show very similar values. The soft phase corresponds to magnetite particles, Phase1 H_{CR} is 37.9 mT and 33.1 mT for HmMgSth1 and HmMgSth2 respectively. Both values are consistent with the H_{CR} found for pure magnetite (37.0 mT) (Table 1). Same coherence is observed for the Phase3 H_{CR} of the hard phase, 949.0 mT and 944.2 mT for both mixed samples, 931.9 mT for pure hematite.

The MDF_{IRM} values were concordant with the soft/hard composition in each sample. The MDF_{IRM} was not reached for HmMgSth1 and this fact agrees with the predominance of a hard phase. On the other hand, the MDF_{IRM} was determined for the sample with a predominant soft phase (HmMgSth2); and its value is close to the one of pure synthetic magnetite (MgSth2).

Finally, in both samples a third phase (Phase2) was obtained with a very low contribution (3.4% and 3.0% respectively). It is possible that these phases have no physical significance, being a product of inaccuracy of the method. Remanent coercivities and S-ratio support this conclusion; both parameters in each sample are biased by Phase3 parameters.

Natural samples

A dominant ferrimagnetic phase (84.0%) was found for PE1a8 sample. This phase is clearly ferrimagnetic because of its remanent coercivity, 31.2 mT. No significant contributions of harder phases were found, (Phase2 H_{CR} = 122.4 mT and Phase3 H_{CR} = 394.9 mT, 8.2% and 7.8% contribution respectively). These results are in agreement with the sample characteristics; this sam-

ple belongs to a polluted layer from a sediment core. Although a quantitative relationship between H_{CR} from Total data and H_{CR} from the individual phases was not established, Total H_{CR} is similar to H_{CR} of the predominant phase, Phase1 H_{CR}, (Fig. 7). In this case S-ratio and H_{CR} are slightly biased by harder magnetic phase contributions, but the S-ratio is less dependent.

The relatively low MDF_{IRM} value, 15.7 mT, for this sample also indicated the predominance of a soft magnetic phase. This parameter is similar to the one for pure synthetic magnetite (MgSth2).

The PE1a12 sample showed a different magnetic behaviour and a relatively balanced contribution was found. Phase1 corresponds to a soft magnetic phase (Phase1 H_{CR} = 38.6 mT) and its contribution is 55.3%. Phases 2 and 3 showed similar remanent coercivities to Phases 2 and 3 from PE1a8 sample; however, they had more significant contributions, about 18.3% and 26.4% respectively. These results agree with MDF_{IRM} parameter (44.6 mT), higher than MDF_{IRM} for PE1a8, and with specific SIRM (1.500E-3 A m^2 kg^{-1}, lower than the SIRM for PE1a8, 1.405E-2 A m^2 kg^{-1}). Phases 2 and 3 for both samples are associated to hard materials, such as hematite and goethite, although S-ratio for Phase2 does not seem to reflect the presence of a hard magnetic phase (Table 1). Total H_{CR} is between Phase1 H_{CR} and Phase2 H_{CR} (Fig. 7).

The GoP2 and PE1a12 samples showed very similar magnetic characteristics. A balanced contribution between phases was found, therefore, Total H_{CR} is also between Phase1 H_{CR} and Phase2 H_{CR} (Fig. 7).

Three magnetic phases for the goethite sample (Goeth1b) were discriminated. In this sample, hard magnetic material dominates the bulk magnetic properties. Phase 3 has the highest contribution, about 75.1%, and its remanent coercivity (Phase3 H_{CR}) is 325.8 mT. Phase2, correspondent to a relatively hard phase (Phase2 H_{CR} = 140.1 mT) may be hematite of 40-75μm (Dankers, 1978), although its S-ratio is too high. A soft magnetic phase, Phase 1 (Phase1 H_{CR} = 73.6 mT), was also found with a no significant contribution, 7.1%. Unlike the other three natural samples, Total H_{CR} is close to the Phase3 H_{CR} (Phase 3, the hardest magnetic phase), (Fig. 7). The predominance of hard material is also supported by the high MDF_{IRM} values, in this case not determined for AF up to 102.5 mT.

The proposed method and related numerical methods

In order to compare the achieved discrimination between different phases, two numerical methods, cumulative log-Gaussian analysis (CLG, Kruiver et al, 2001a) and Irmunmix method (UM, Heslop et al, 2002) were used. Both methods decompose bulk IRM acquisition curves into a number of IRM components (defined by the user) by numerical analysis. Such individual components have a log-normal distribution (Robertson and France, 1994), and they are characterised by the intrinsic features of each magnetic carrier population, such as SIRM or contribution to the bulk IRM acquisition curve, mean $H_{1/2}$ and dispersion (DP).

CLG analysis involves three combined studies of a linear acquisition plot (LAP), a gradient of acquisition plot (GAP) and a standardised acquisition plot (SAP). The fitting procedure in this technique requires an interactive work of the user, obtaining better fittings minimising the magnitude of residual between the data and modelled curves. On the other hand, Irmunmix is an automated fitting method based on expectation-maximisation algorithm that requires starting settings to reach a final fitting model. SIRM, mean $H_{1/2}$ and DP for each component are obtained from both methods. Deconvolution of the first derivative curve into contributing (normal distribution) curves can yield various comparative results; i.e. decomposition of two and three components can be both appropriate to model a measured curve. In order to determine whether an interpretation is significantly better (at a specified level of significance) than the other one, two statistics tests (F-test and t-test) can be used.

Experimental parameters, contribution to the Total IRM and mean $H_{1/2}$, from discriminated phases by using our method were used in CLG method. Only the DP parameter was fitted in order to obtain a separation between components and modelled the measured data. Results of the three parameters for each component are summarised in Table 3. Fitting for each numerical method, using only the measured Total IRM, was carried out regarding two possibilities, fit1 (three components) and fit2 (two components) (Table 3).

All samples were discriminated between three experimental phases (except MgSth2 sample) and the fitting was calculated using three components (fit1) and two-one components (fit2). For each numerical method, fit1 was statistically compared against fit2. F-test and t-test results are given in Table 4. These results are compared with critical values for a confidence value of 95%, critical F-value for N = 25 is 1.84 and critical t value for N = 50 is 1.68. F-test is firstly applied and then if it is necessary t-test. In both cases the variance of squared residuals is compared; the smallest one is interpreted as the best fit. In several cases both fits are statistically similar and both interpretations are possible. In other cases there are no differences for two analyses (e.g. LAP and GAP, MgSth2 sample, Table 4) and other results are conclusive (SAP, MgSth2 sample). There is no agreement between analyses for three samples, e.g. HmMgSth2 sample, fit1 is better according

Table 3. Results of individual IRM acquisition curves for the experimental and two numerical methods. For numerical methods two fitting (fit1 and fit2) are tried.

Tabla 3. *Resultados de las curvas de MRI de adquisición para el método experimental y los dos numéricos (CLG y UM). Para los métodos numéricos se probaron dos ajustes (fit1 y fit2).*

	Parameters from each individual IRM acquisition curves								
	Phase1			Phase2			Phase3		
Sample	contribution	$H_{1/2}$	DP	contribution	$H_{1/2}$	DP	contribution	$H_{1/2}$	DP
	(%)	*(mT)*	*(log mT)*	*(%)*	*(mT)*	*(log mT)*	*(%)*	*(mT)*	*(log mT)*
MgSth2 (EM)	99,3	73,9	0,31	0,7	128,8	1,00	—	—	—
fit1 (CLG)	93,5	69,2	0,29	—	—	—	6,5	1584,9	0,12
fit2 (CLG)	100,0	70,8	0,30	—	—	—	—	—	—
fit1 (UM)	93,4	70,8	0,31	—	—	—	6,6	1595,9	0,15
fit2 (UM)	89,6	69,4	0,30	3,4	163,9	0,25	6,9	1528,6	0,17
HmSth3 (EM)	5,2	546,5	0,40	5,2	437,3	0,45	89,6	1083,2	0,27
fit1 (CLG)	0,4	158,5	0,50	7,4	316,2	0,29	92,2	1148,2	0,29
fit2 (CLG)	—	—	—	2,0	199,5	0,37	98,0	1148,2	0,33
fit1 (UM)	4,8	332,3	0,25	3,0	790,7	0,62	92,1	1255,2	0,32
fit2 (UM)	—	—	—	—	—	—	100,0	1288,2	0,38
HmMgSth1 (EM)	32,6	61,7	0,35	3,4	391,3	0,35	63,9	1091,4	0,23
fit1 (CLG)	28,8	58,9	0,33	3,2	316,2	0,20	67,9	1148,2	0,25
fit2 (CLG)	29,3	57,5	0,32	—	—	—	70,7	1096,5	0,26
fit1 (UM)	24,5	52,7	0,28	3,8	297,2	0,13	71,6	1235,1	0,29
fit2 (UM)	23,1	52,3	0,28	—	—	—	76,9	1252,0	0,35
HmMgSth2 (EM)	64,2	57,6	0,30	3,0	527,2	0,50	32,8	1054,9	0,25
fit1 (CLG)	60,9	56,2	0,27	1,5	316,2	0,15	37,6	1122,0	0,27
fit2 (CLG)	60,4	55,0	0,28	—	—	—	39,6	1071,5	0,29
fit1 (UM)	57,0	54,8	0,28	2,7	658,6	0,19	40,2	1238,8	0,33
fit2 (UM)	57,3	54,7	0,28	—	—	—	42,7	1154,5	0,33
PE1a8 (EM)	84,0	44,8	0,35	8,2	133,3	0,30	7,7	355,9	0,55
fit1 (CLG)	89,6	47,9	0,36	7,0	158,5	0,36	3,5	1258,9	0,40
fit2 (CLG)	96,5	52,5	0,39	—	—	—	3,5	1412,5	0,34
fit1 (UM)	88,5	47,9	0,35	10,5	204,8	0,38	1,0	1679,6	0,07
fit2 (UM)	96,6	52,8	0,37	—	—	—	3,3	813,0	0,28
PE1a12 (EM)	55,4	47,6	0,35	18,2	123,3	0,20	26,4	342,6	0,50
fit1 (CLG)	53,2	56,2	0,45	41,6	125,9	0,35	5,2	1584,9	0,15
fit2 (CLG)	95,7	85,1	0,47	—	—	—	4,3	1659,6	0,16
fit1 (UM)	64,9	63,9	0,42	32,0	167,3	0,40	3,1	1686,2	0,10
fit2 (UM)	96,8	87,6	0,46	—	—	—	3,2	1678,4	0,11
GoP2 (EM)	58,1	51,2	0,37	19,6	125,0	0,18	22,2	299,7	0,41
fit1 (CLG)	56,6	55,0	0,39	23,7	128,8	0,24	19,7	299,7	0,60
fit2 (CLG)	97,4	85,1	0,45	—	—	—	2,6	1584,9	0,20
fit1 (UM)	53,1	63,4	0,43	44,2	122,6	0,36	2,7	1384,2	0,18
fit2 (UM)	100,0	92,3	0,47	—	—	—	—	—	—
Goeth1b (EM)	7,1	77,9	0,30	17,7	138,8	0,15	75,2	333,3	0,25
fit1 (CLG)	2,8	66,1	0,28	93,5	269,2	0,28	3,8	1584,9	0,20
fit2 (CLG)	—	—	—	97,5	257,0	0,29	2,5	1778,3	0,10
fit1 (UM)	—	—	—	84,8	255,1	0,27	15,1	568,2	0,61
fit2 (UM)	—	—	—	—	—	—	100,0	270,5	0,32

Experimental Method (EM), Cumulative log-Gaussian analysis Method (CLG), Unmix Method (UM).

to LAP and fit2 is better according to SAP analysis. Cases of no agreement between methods are also found, e.g. PE1a8. Although it is possible to decide the best fit, disagreement between analyses or methods are observed and additional information is necessary to remove the ambiguity. It is also necessary to take into account the magnitude of the contribution of each phase. Low contribution can be misinterpreted, e.g. in MgSth2 sample only magnetite is present, however, a hard phase is observed from numerical methods. Possibly, according to the low contributions (around 6%), the existence of this phase constitutes an artifact.

Parameters of experimental phases agree with fit1 (three components) better than with fit 2. Contribution values for experimental phases also agree well with fit1. Nevertheless, some differences are found in two natural samples, PE1a12 and Goeth1b. Statistics test is not conclusive for sample PE1a12; ambiguous results and no differences between fit1 and fit2 are obtained, i.e. measured data can be modelled using either three or two components and therefore two interpretations are possible. For Goeth1b sample, fit1 is better than fit2 and therefore a higher number of components is favoured (three components better than two for CLG method and two components better than one for UM method). Nevertheless, component 2 obtained by CLG and UM seems to contain the phases2 and 3 discriminated by our method (Table 3).

Overlapping coercivity curves can be present in these samples and therefore numerical methods might not be able to separate them into individual curves. Another possibility can be related to errors in measurements or, in the case of the Goeth1b sample, a split of the main phase can be a consequence of a slight intensity decrease at high AF (Fig. 1).

Advantages and disadvantages of the method

As discussed before, successful results were obtained in samples of well-known pure and mixed synthetic magnetic material. However, it is necessary to have a critical view to analyse the results, especially for cases where phases with low contributions are present. It is necessary to evaluate whether the values of magnetic parameters of the minor phase are consistent. For the studied synthetic samples, the minor phases may not be real, due to various factors, such as, inaccuracy of the method, measurement errors, time dependence of IRM (Worm, 1999), interaction between magnetic grains, etc.

Regarding the inaccuracy of the method, it could lead to not well defined phases. This difficulty may be detected by incompatibilities between values of related magnetic parameters, such as S-ratio and H_{CR}. This effect was mainly observed in minority phases and it is more often when hard (antiferromagnetic) minerals are the main contributions to the magnetic signal. It may be related to the partial reduction of remanent magnetisation of some hard minerals when they are subject to AFs about 100 mT during AF demagnetisation (Fig. 1).

Using this method in natural samples, it was possible to discriminate magnetic phases that could not be observed by using numerical methods because they have overlapped coercivities. As mentioned above, we could not clearly distinguish three magnetic phases in two natural samples from numerical analyses (Table 4).

A real advantage of this method arising from backfield IRM is that two important parameters (H_{CR} and S-ratio) for *each* phase can be obtained, which cannot be determined by other methods. The reliability of these magnetic parameters is specially supported from mixing synthetic sample results. H_{CR} and S-ratio for each main phase agree well with magnetic parameters of unmixed synthetic samples.

Empirical relations

In spite of the fact that H_{CR} and $H_{1/2}$ are equal for an assembly of homogeneously distributed and randomly oriented single domain grains (Wohlfarth, 1958), this relationship is not necessarily true for natural samples and samples containing an assortment of domain grains (e.g. pseudo-single domain and multidomain grains). Differences between both parameters can be mainly derived from the interacting field between grains, hence H_{CR} slightly decreases and $H_{1/2}$ increases (Dankers, 1981).

Although these parameters are obtained from two different connected measurements (back-field IRM and IRM acquisition curves) and they have differences, both are functionally related. A linkage between them (equation (2)) was tried to establish from the obtained results (N=27) summarised in Tables 1 and 2. From the study of linear regression fit, a very good correlation between both parameters was found, R=0.996 (Fig. 8). The following linear relationship was found,

$$H_{CR} = 0.88 * H_{1/2} \qquad (2)$$

and therefore, $H_{CR}/H_{1/2} = 0.88 \pm 0.01$ for total and individual phases. Dankers (1981) found a similar relationship between magnetic parameters from a number of specimens containing natural magnetite, titanomagnetite and hematite of different grain size. Relationship especially expressed as the $H_{CR}/H_{1/2}$ ratio was established for each kind of mineral. He found ratios close to 1 for hematites, around 0.62 (varying from 0.55 to 0.71) for magnetites and around 0.83 (varying between 0.71 and 1) for titanomagnetites. Magnetite grains used in such study ranged between

Table 4. Statistics, *F*-tests and *t*-test, for two interpretations (fit1 and fit2) for each numerical method.

Tabla 4. *Pruebas estadísticas, prueba-F y prueba-t, para las dos interpretaciones (fit1 y fit2) para cada método numérico (CLG y UM).*

Sample			*F*-test	*t*-test	Test results
MgSth2	fit1 and fit2 (CLG)	LAP	1,03	1,54	No difference
		GAP	1,51	0,38	No difference
		SAP	231,78		fit1 better
	fit1 and fit2 (UM)	LAP	1,50	0,21	No difference
		GAP	1,09	0,03	No difference
		SAP	1,23	0,16	No difference
HmSth3	fit1 and fit2 (CLG)	LAP	4,07		fit1 better
		GAP	1,42	0,09	No difference
		SAP	29,35		fit1 better
	fit1 and fit2 (UM)	LAP	3,13		fit1 better
		GAP	1,16	0,32	No difference
		SAP	781,14		fit1 better
HmMgSth1	fit1 and fit2 (CLG)	LAP	210,49		fit1 better
		GAP	1,82	0,29	No difference
		SAP	2,10		fit1 better
	fit1 and fit2 (UM)	LAP	4,12		fit1 better
		GAP	1,10	0,36	No difference
		SAP	1,03	0,00	No difference
HmMgSth2	fit1 and fit2 (CLG)	LAP	4,61		fit1 better
		GAP	1,01	0,09	No difference
		SAP	2,13		fit2 better
	fit1 and fit2 (UM)	LAP	1,46	0,67	No difference
		GAP	1,07	0,05	No difference
		SAP	1,24	0,09	No difference
PE1a8	fit1 and fit2 (CLG)	LAP	2,91		fit2 better
		GAP	1,70	0,31	No difference
		SAP	1,78	0,11	No difference
	fit1 and fit2 (UM)	LAP	14,67		fit1 better
		GAP	1,83	0,45	No difference
		SAP	1,73	0,89	No difference
PE1a12	fit1 and fit2 (CLG)	LAP	9,00		fit2 better
		GAP	1,12	0,20	No difference
		SAP	1,95		fit1 better
	fit1 and fit2 (UM)	LAP	1,35	0,26	No difference
		GAP	1,13	0,13	No difference
		SAP	1,79	0,31	No difference
GoP2	fit1 and fit2 (CLG)	LAP	4,69		fit1 better
		GAP	1,33	0,24	No difference
		SAP	1,57	0,16	No difference
	fit1 and fit2 (UM)	LAP	10,31		fit1 better
		GAP	2,05		fit1 better
		SAP	4,46		fit1 better
Goeth1b	fit1 and fit2 (CLG)	LAP	2,51		fit1 better
		GAP	1,32	0,17	No difference
		SAP	8,19		fit1 better
	fit1 and fit2 (UM)	LAP	3,67		fit2 better
		GAP	6,02		fit1 better
		SAP	6,59		fit1 better

For a confidence level of 95%, critical F value for N = 25 is 1,84 and critical t value for N = 50 is 1,68. Cumulative log-Gaussian analysis (CLG), Linear acquisition plot (LAP), gradient of acquisition plot (GAP), stan-plot (SAP). Unmix Method (UM)

5 and 250μm (PSD and MD grains). On the other hand, Dunlop (1986) extended the grain size range of magnetite studying submicron magnetites, ranging between 0.04 and 0.22μm (SD and PSD grains). He obtained $H_{CR}/H_{1/2}$ ratios varying from 0.67 to 0.80. According to both studies, this ratio increases from MD to PSD to SD grains, and they give an entire magnetite interval that ranges from 0.55 to 0.80.

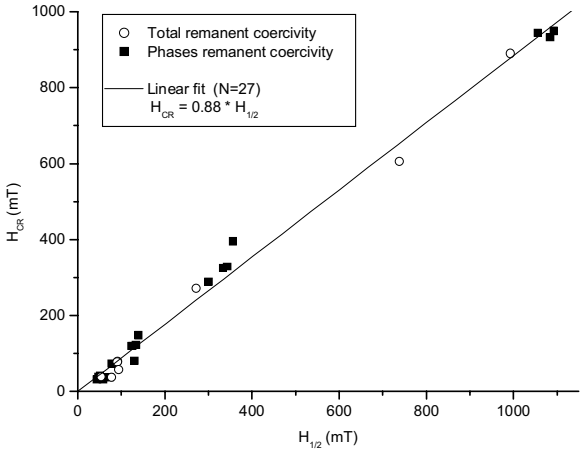

Figure 8 – Remanent coercivity (H_{CR}) vs remanent coercivity acquisition ($H_{1/2}$) for Total and Phases data from all samples, synthetic and natural samples.

Figura 8 – *Coercitividad remanente (H_{CR}) versus coercitividad remanente de adquisición ($H_{1/2}$) para datos de Fases y Totales de todas las muestras (sintéticas y naturales).*

The proposed relationship (equation 2) agrees very well with results obtained by Dankers (1981) and Dunlop (1986). It should be taken into account that the data used in our linear fit are "pure"and mixed samples involving magnetites, maybe titanomagnetites, hematites and goethites. Therefore such relationship (equation 2) might have a more global character. $H_{CR}/H_{1/2}$ ratios from individual soft and hard phases show differences inbetween, that are supported by the above mentioned interval of coercitivity values for magnetite, titanomagnetite and hematite. It is worth mentioning that Total $H_{CR}/H_{1/2}$ ratios (as well as other ratios, e.g. S-ratio) of mixed samples are influenced by contribution of soft/hard materials, i.e. $H_{CR}/H_{1/2}$ is 0.82 for a magnetically harder sample (HmMgSth1), and on the other hand, 0.61 for a magnetically softer sample (HmMgSth2).

Remarks for the proposed method

From these results we can see that the research on the proposed method must go further in order to improve it. Variables to be taken into account are related with AF demagnetisation; one of them is the selected peak AF value, which determines the AF filter because the response of each mineral and their different grain size is different. Other variable is the AF decay rate for the *tumbling method* (Dankers, 1978; Egli and Lowrie, 2002). If AF is not slowly reduced to zero, and the specimen is not quickly rotated, the remanence with coercivities lower than the peak AF might not be cancelled out randomly. Therefore some directions might not be suitably swept and consequently the intensity of remanent magnetisation will be affected. The above mentioned inaccuracy for several non-significant contributions of Phases could be removed if these variables are taken into account.

If the saturation of magnetically hard minerals is not reached, it might be difficult to calculate some parameters from its corresponding phase, especially $H_{1/2}$ and SIRM because they can be underestimated. However, such problem can only arise for hard materials (especially goethite and hematite), so this difficulty can be solved using higher pulse magnetising fields and rearranging the growing field steps. On the other hand, discrimination itself can be successfully carried out even if the hard phase has not reached its saturation remanence.

From section 5.3, it is possible to conclude that there is satisfactory agreement between the *experimental method* and numerical methods. The experimental method is more time-consuming than the other. However, this method provides an *experimental* and therefore, a more *realistic* discrimination into individual phases contributing to Total IRM curve.

Finally, we think that fruitful results can be obtained using alternatively the experimental and numerical methods. For instance, the experimental method might be applied to pilot samples and information about the expected number of individual contributing curves can be obtained. Then this extra information can be taken into account in order to model IRM curves for the rest of samples by using numerical methods.

Another interesting possibility is the joint use of both kind of methods, i.e. experimental method can be used to discriminate main phases and then numerical methods can be applied to each phase or residual curve in order to investigate it in a more detailed way.

CONCLUSIONS

The experimental method is suitable to separate hard and soft magnetic phases for samples containing pure synthetic magnetite and hematite and a different composition of them and several natural magnetic minerals. Such ability is tested specially from mixing samples. Measured individual IRM curves for mixtures are in agreement with predicted results calculated from the known ratios of the samples and their corresponding SIRM values of "pure" samples. Using the method it was possible to discriminate mag-

netic phases in natural samples that could not be observed by using other methods, at least without additional information.

A linear relationship between remanent coercivities, H_{CR} and $H_{1/2}$, was established for every phase. The calculated slope from equation 2 (or $H_{CR}/H_{1/2} = 0.88$) involves data of soft/hard phases and both of them, hence it is interpreted as a global result. It is worth mentioning that $H_{CR}/H_{1/2}$ ratio for individual phases corresponds to characteristic values according to Dankers (1981) and Dunlop (1986).

The method was carried out using two peak AF values of 50 and 102.5 mT as a first try. Different or more convenient peak AF values could be selected, in order to discriminate minerals with another coercivity spectrum and also to improve separation between phases. In order to achieve improvements for the method, it will be necessary to research the effect of several AF demagnetisation variables in an exhaustive way, such as peak AF, decay rate of AF, etc.

The discrimination obtained using our *experimental method* agrees with results obtained from purely numerical methods. Although our experimental method is more time-consuming than others, it provides an experimental and realistic discrimination into individual phases contributing to the Total IRM measurements.

This method is also successfully applied to backfield IRM measurements, obtaining S-ratios and H_{CR} parameters for each phase that cannot be determined by other methods. The reliability of S-ratio and H_{CR} is supported by the results of mixing synthetic samples, since the results for each main phase agree with those obtained for unmixed synthetic samples.

ACKNOWLEDGEMENTS

The authors wish to thank the Universidad Nacional del Centro de la Provincia de Buenos Aires (UNCPBA) and CONICET for financial support. Many thanks to C. Vasquez and J. C. Bidegain for the provided samples.

The authors are really indebted to the anonymous reviewer for his useful commentaries and suggestions.

REFERENCES

ARGYLE KS, DUNLOP DJ and XU S. 1994. Single-domain behaviour of multidomain magnetite grains. Abstract Eos (Trans. Am. Geophys. Un.), 75, Fall Meeting suppl., 196.

BAILEY ME and DUNLOP DJ. 1983. Alternating field characteristics of pseudo-single domain (2-14μm) and multidomain magnetite. Earth Planet. Sci. Lett., 63: 335–352.

BLOEMENDAL J, KING JK, HALL FR and DOH SJ. 1992. Rock magnetism of Late Neogene and Pleistocene deep-sea sediments: Relationship to sediment source, diagenetic processes and sediment lithology. J. Geophys. Res., 97: 4361–4375.

CHAPARRO MAE, BIDEGAIN JC, SINITO AM, GOGORZA CS and JURADO S. 2002a. Preliminary Results of Magnetic Measurements on Stream-Sediments from Buenos Aires province, Argentina. Studia Geophysica et Geodaectia, 47(1): 121–145.

CHAPARRO MAE, BIDEGAIN JC, SINITO AM, GOGORZA CS and JURADO S. 2002b. Comparison of Magnetic Studies of Soils and Stream-Sediments from Buenos Aires Province (Argentina) Applied to Pollution Analysis. Extended abstract for the International Symposium on Fundamental Rock Magnetism and Environmental Applications. Erice, Italy, 25–27.

CHAPARRO MAE, SINITO AM and BIDEGAIN JC. 2003. Estudios Magnéticos sobre Goethita (α-FeOOH) Natural de Tharsis (Huelva, España). Boletin Geológico y Minero Español, (submitted).

DANKERS PHM. 1978. Magnetic properties of dispersed natural iron-oxides of known grain-size, thesis, State University of Utrecht, 142 pp.

DANKERS PHM. 1981. Relationship between median destructive field and remanent coercive forces for dispersed natural magnetite, titanomagnetite and hematite. Geophys. J. R. Astr. Soc., 64: 447–461.

DE BOER CB and DEKKERS MJ. 1998. Thermomagnetic behaviour of hematite and goethite as a function of grain size in various non-saturating magnetic fields. Geophys. J. Int., 133: 541–552.

DUNLOP DJ. 1986. Coercive forces and coercivity spectra of submicron magnetites. Earth and Planet. Sci. Lett., 78: 288–295.

DUNLOP DJ and ÖZDEMIR Ö. 1997. Rock magnetism. Fundamentals and frontiers. Cambridge University Press. 573 pp.

EGLI R and LOWRIE W. 2002. Anhysteric remanent magnetization of fine magnetic particles. J. Geophys. Res., 107(B10): 2209, doi: 10.1029/2001JB000671.

FRANCE DE and OLDFIELD F. 2000. Identifying goethite and hematite from rock magnetic measurements of soils and sediments. J. Geophys. Res., 105 (B2): 2781–2795.

HESLOP D, DEKKERS MJ, KRUIVER PP and VAN OORSCHOT IHM. 2002. Analysis of isothermal remanent magnetisation acquisition curves using the expectation-maximisation algorithm. Geophys. J. Int., 148: 58–64.

KRUIVER PP, DEKKERS MJ and HESLOP D. 2001a. Quantification of magnetic coercivity components by the analysis of acquisition curves of isothermal remanent magnetisation. Earth and Planet. Sci. Lett., 189: 269–276.

KRUIVER PP and PASSIER HF. 2001b. Coercivity analysis of magnetic phases in sapropel S1 related to variations in redox conditions, including

an investigation of the S ratio. Geochem. Geophys. and Geosys. Paper number 2001GC000181.

MAHER BA, THOMPSON R and HOUNSLOW MW. 1999. Introduction. In: Quaternary Climate, Environments and Magnetism (Maher B.A. and Thompson R., eds.), 1-48 pp. Cambridge University Press, Cambridge.

PETERS C and THOMPSON R. 1998. Magnetic identification of selected natural iron oxides and sulphides. J. Magn. Magn. Mater., 183: 365–374.

PETERS C, DEKKERS MJ and LANGEREIS CG. 2002. Validation of mineral magnetic methods. Extended abstract for the International Symposium on Fundamental Rock Magnetism and Environmental Applications. Erice, Italy, 129–130.

ROBERTSON DJ and FRANCE DE. 1994. Discrimination of remanence-carrying minerals in mixtures using isothermal remanent magnetization acquisition curves. Phys. Earth Planet. Int., 82: 223–234.

STOCKHAUSEN H. 1998. Some new aspects for the modelling of isothermal remanent magnetization acquisition curves by cumulative log Gaussian functions. Geophys. Res. Lett., 25 (12): 2217–2220.

THOMPSON R and OLDFIELD F. 1986. Environmental magnetism. Allen & Unwin (Publishers) Ltd., 225 pp.

WOHLFARTH EP. 1958. Relations between different modes of acquisition of the remanent magnetization of ferromagnetic particles. J. Appl. Phys., 29: 595–596.

WORM HU. 1999. Time-dependent IRM: A new technique for magnetic granulometry. Geophysical Res. Ltrs. 1999GL008360, 26 (16): 2,557.

XU S and DUNLOP DJ. 1995. Towards a better understanding of the Lowrie-Fuller test. J. Geophys. Res., 100: 22,533–22,542.

NOTES ABOUT THE AUTHORS

Marcos Adrián Eduardo Chaparro was born on April 17th 1972 in San Cayetano (Argentina); he began his research in physics in 1996 before he obtained his M.Sc. degree in Physics in Nov 1999. After on, he began his PhD studies in Physics and has been actively involved in Geomagnetism research, namely magnetic signature of anthropogenic pollution in river sediments and soils. Current Position: Teaching Assistance, Facultad de Ciencias Exactas, UNCPBA. Postgraduate Fellow of National Council of Scientific and Technical Research of Argentina (CONICET). Research Interest: Environmental magnetism, Magnetic properties of materials, Experimental Methods of Rock-magnetism. Paleomagnetism on lake sediments.
Web site: http://www.exa.unicen.edu.ar/ifas/paleomag.html

Ana María Sinito was born on February 14, 1950 (Buenos Aires, Argentina), Argentine Citizen, married, two children. Degrees: Master in Physics – Universidad de Buenos Aires, Argentina, 1973. Ph.D. in Physics – Universidad de Buenos Aires, Argentina, 1988. Current Position: Full Professor, Facultad de Ciencias Exactas – UNCPBA. Principal Researcher, CONICET (National Council of Scientific and Technical Investigations). Director of the Institute of Physics "Arroyo Seco" (IFAS) of the UNCPBA, 10/1/1999 until now. Secretary of the Sub-committee of Geomagnetism and Aeronomy of the National Committee of IUGG, 12/6/2000 until now. Fields of currents interests: Paleomagnetism on lake sediments, paleosecular variations and reversals of geomagnetic field. Environmental magnetism, anthropogenic pollution.